A Miniaturized Prototype for Continuous Noninvasive Transcutaneous Oxygen Monitoring

Burak Kahraman*[‡], Vladimir Vakhter*[‡], Ian Costanzo*, Guixue Bu[†], Foroohar Foroozan[†], and Ulkuhan Guler*

*Department of Electrical and Computer Engineering, Worcester Polytechnic Institute, Worcester, MA 01609 USA

†Analog Devices Inc., Wilmington, MA 01887 USA

Abstract—Luminescent oxygen sensing is employed for measuring the partial pressure of oxygen diffusing through the skin, named transcutaneous oxygen. Two well-known approaches are intensity- and lifetime-based measurement for assessing transcutaneous oxygen. The lifetime-based technique is preferable as it offers lower susceptibility to optical path changes and reflections compared to the intensity-based method. High-resolution lifetime capturing is critical to accurate transcutaneous oxygen measurements from the human body. This study proposes a miniaturized prototype based on a multimodal analog front end, ADPD4101, and a custom firmware. We have demonstrated that the prototype could detect small changes in the lifetime with high resolution, showing its suitability for future human subject tests. We implemented the prototype on a 68 mm \times 43 mm printed circuit board (PCB) and consumes the power of 39 mW.

I. INTRODUCTION

The growing interest in remote diagnostic and therapy creates a demand for the next generation of smart and connected health devices [1]. The variety of applications, use cases, and novel designs allow classifying them as an emerging technologies. As depicted in Fig. 1, these devices can create a cost-efficient, easy-access, flexible, and proactive healthcare model. For example, chronic diseases caused 55% of deaths in the United States in 2017 [2]. Wearable devices can potentially reduced this mortality rate by detecting symptoms in the early phase if a patient can be monitored continuously and remotely [3].

While popular consumer devices (e.g., the Fitbit tracker [4]) measure the user's physical activity and vital signs throughout the day, they are known not to be precise for medical purposes [5]. Some wearables [6]–[8] have explicitly emerged for medical applications. For instance, SensiumVitals [6] allows healthcare teams to monitor the patient's body temperature and heart rate continuously after discharge from surgical intensive care units (SICUs) [6]. With such devices, medical professionals are invisioned to have the ability to detect anomalies in patient's vital signs early on [9], [10].

Although medical wearable technologies have gone through significant advancements, there is a limitation in both the variety and the quality of the vital signs they provide. Furthermore, amid this transformation, there has been little progress

Burak Kahraman[‡] and Vladimir Vakhter[‡] contributed equally to this work. This material is based upon work supported in part by the National Science Foundation (NSF) under Grant EECS-2143898 and Analog Devices Inc. (ADI) through a research gift. Corresponding author: Ulkuhan Guler: uguler@wpi.edu.

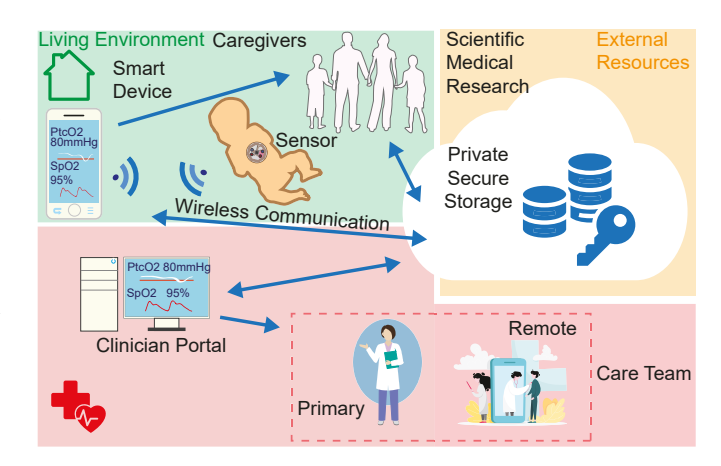


Fig. 1. Remote patient monitoring with smart wearable devices.

in miniaturizing respiration-sensing devices to a compact form factor [11]. Yet, respiration parameters are critical to assessing human health [12].

The arterial partial pressure of oxygen (PaO₂) and carbon dioxide (PaCO₂) are vital respiration parameters to asses the gas exchange in the lungs during the respiration cycle as they describe the transfer of O2 and CO2 across the bloodair barrier between the alveoli and the bloodstream [13], [14]. Therefore, the PaO₂ data are valuable for detecting acute and chronic respiratory diseases such as chronic obstructive pulmonary disease (COPD) and emphysema [15], [16]. Although the standard method of assessing PaO₂ is arterial blood gas analysis [17], it is unsuitable for continuous monitoring as it is invasive and painful. However, a noninvasive surrogate method to continuously assess PaO₂ by measuring transcutaneous partial pressure of oxygen exists. This method monitors the partial pressure of oxygen on the skin (PtcO₂). Recently, the luminescent oxygen sensing technique employing a film sensitive to oxygen has been explored to measure PtcO2 with miniaturized devices [18]-[20].

This paper presents a novel ${\rm PtcO_2}$ monitoring prototype based on the luminescent oxygen sensing technique with hardware-software integration. Section II explains the principle of luminescent oxygen sensing and two measurement methodologies. Section III describes the prototype at both the hardware and software levels. Section IV demonstrates the experimental setup used to collect the data presented in Section V. Finally, Section VI concludes the paper.

II. SENSING PRINCIPLE

The key elements employed in the luminescent oxygen sensing technique are a blue light-emitting diode (LED), a longpass or band-pass optical filter, a red photodiode (PD), and a luminescent sensing film composed of platinum porphyrin (Ptporphyrin). A blue LED with a peak emission wavelength (λ) of 450 nm is used to excite the luminescent sensing film. When the sensing film is excited, luminophore molecules inside the sensing film make transition from their ground state to a higher energy state. After a short transition from the higher energy state to an intermediate state, the luminophore molecules re-emit a photon and relax to their ground state. The re-emitted photon with a λ of 650 nm is then detected by the PD. In this process, oxygen acts as a quencher. When luminophore molecules interact with oxygen molecules, the excited luminophore molecules transfer some of their energy to the oxygen molecules. This action reduces the intensity and lifetime of the re-emitted red light. Thus, this process leads to an inverse relationship between the intensity and lifetime of re-emitted photons and the partial pressure of oxygen (PO₂). Therefore, researchers estimate PO₂ by measuring either the intensity or lifetime of the re-emitted red photons [20]–[22]. In state-of-the-art devices, the photocurrent in a PD, matching the exponential decay curve and intensity of photons, is measured by various types of analog front ends (AFEs) [23]–[25].

A. Intensity-based Method

The amount of re-emitted photons is quantified by luminescent intensity [26]. The luminescent intensity is quenched in proportion to the oxygen molecules in the environment. The method that relates the luminescence intensity to PO_2 is called intensity-based measurements. However, this method is not robust against optical path changes and reflections, changing the measured intensity value and affecting the accurate measurement of PO_2 [25], [27].

B. Lifetime-based Method

The luminescence lifetime expresses the average amount of time luminophore molecules spend in the higher energy state due to excitation [28]. This is a random process: some luminophore molecules spend more time than the average lifetime, while others spend less time. The method that relates luminescence lifetime to PO_2 is called lifetime-based measurements. The lifetime-based method [29] is more robust against optical path changes and reflections compared to the intensity-based method [20], [22]. Therefore, this method is our to-go choice for this prototype aimed at human subject tests.

III. SYSTEM DESIGN

The entire system can be broken down into three parts: (1) the sensor head, from which the optical response is obtained, (2) the electronics which process this optical response to an electrical signal, and (3) the software for processing captured signal and estimating lifetime (τ) from this signal, quantifying PO_2 .

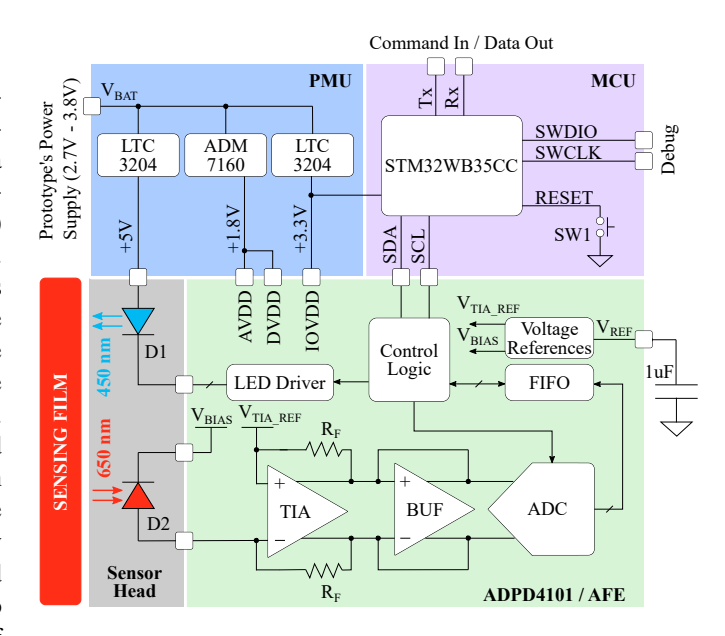


Fig. 2. Top-level diagram of luminescent oxygen-sensing-based $\rm PtcO_2$ monitoring prototype.

A. Hardware Design

The PtcO₂ monitoring prototype consists of three main blocks: (1) power management unit (PMU), (2) microcontroller unit (MCU), and (3) AFE. Fig. 2 demonstrates the top-level diagram of the prototype. The PMU comprises one low-dropout (LDO) regulator (ADM7160, Analog Devices Inc. (ADI)) and two charge pumps (LTC3204, ADI). The first regulator delivers a stable supply voltage of 1.8 V to power up the AFE, whereas the two charge pumps generate stable 3.3 V and 5 V supplies, respectively. The former is used to power up the onboard MCU. The latter is used to drive the LED. We employed a sampling method called impulse response mode to measure the lifetime [30]. In this mode, we pulse the LED once to excite the sensor, and sample the luminescent decay curve in a period called acquisition width.

We employed a multimodal photometric AFE (ADPD4101, ADI) [31]. ADPD4101 has eight integrated LED drivers to stimulate the onboard LEDs and two channels to measure sensor readings. The maximum LED current can be set to 400 mA. The PD is connected to one of the channels of the AFE in a single-ended fashion. The analog signal path of the connected channel includes a transimpedance amplifier (TIA), which converts photocurrent into a voltage, and a buffer, which feds this analog signal to an analog-to-digital converter (ADC). The internally generated voltages V_{TIA_REF} and V_{BIAS} are used to bias the noninverting terminal of TIA and reverse bias the PD, respectively. The gain of TIA is adjustable with a programmable feedback resistor (R_F) . The analog signal fed by the buffer is digitized with the integrated ADC in the ADPD4101. Then, the sampled data is written to a first-infirst-out (FIFO) memory buffer.

The STM32WB35CC 32-bit Arm Cortex-M4 MCU by STMicroelectronics has been used to: (1) configure the AFE for driving the LED; (2) record the signal from the PD; and

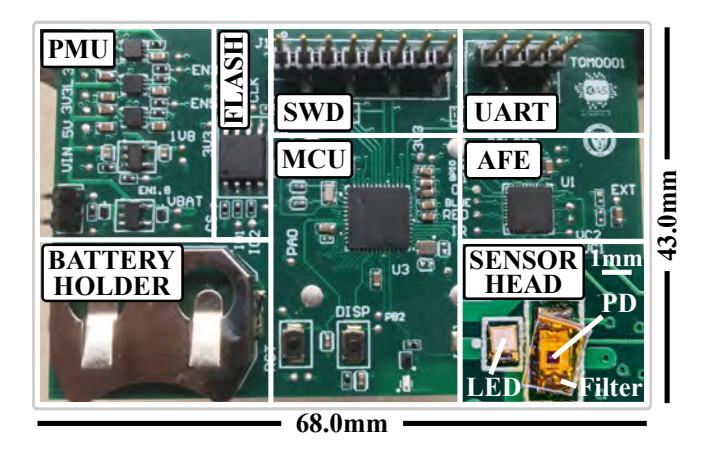


Fig. 3. PCB for PtcO2 monitoring based on luminescent oxygen sensing.

(3) transmit the experimental data to the computer. The MCU's hardware reset functionality is provided by connecting the SW1 switch to the V_{RESET} pin. The MCU is programmed via the serial wire debug (SWD) port. The MCU and the AFE communicate via the Inter-Integrated Circuit (I2C) bus. The MCU reads the data out from the FIFO of the ADPD4101. Then, these data are sent to the computer (PC) via the universal asynchronous receiver-transmitter (UART) interface to calculate τ .

B. Firmware Design

This subsection provides an overview of the current firmware controlling our PtcO₂ monitoring prototype. The host MCU runs bare-metal firmware that provides low-level hardware control and also reduces the memory overhead and the power consumption. This firmware has the so-called "super-loop" architecture. In this architecture, the initialization routines precede an infinite loop where all the primary tasks of the system are contained except for several interrupt service routines (ISR) or interrupt handlers. There are two hardware interrupt handlers (ISR 1 and ISR 2) and one timer-interrupt handler (ISR 3). ISR 1 is invoked when the AFE generates a falling edge on its GPIO0 pin, indicating that its FIFO buffer contains the desired amount of samples. ISR 2 handles the display button press event. ISR 3 is called when a system timer's period has elapsed.

During the initialization phase, the firmware configures the MCU (memory, system clock, communication interfaces, input/output ports, etc.). Then, the MCU establishes a connection with the AFE via I2C. After that, the MCU loads a configuration file into the AFE and puts it into the GO (sampling) mode. The main loop checks the status of the dataready flag set by ISR 1. If the flag is set, it puts the AFE into the IDLE (standby) mode and reads out the data available in the AFE's FIFO. When the data are read, the MCU parses it, stores the parsed values into an array, and updates the variables controlling the parsing of the following data sets. After that, it puts the AFE back into the GO mode. The main loop stops its operation after a given number of decay curves have been collected and averaged to produce the final result.

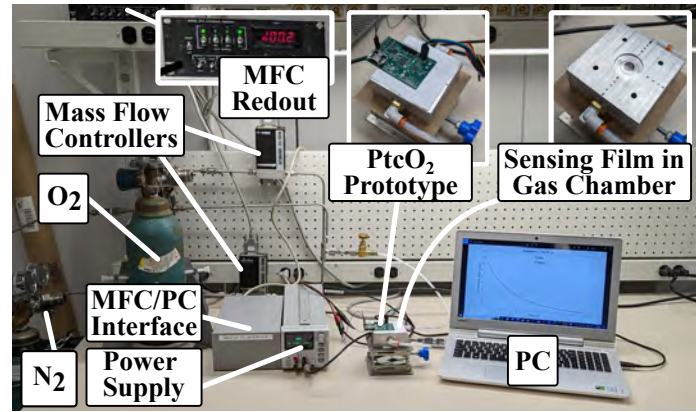


Fig. 4. Gas experiment physical testbench.

IV. EXPERIMENTAL SETUP

We implemented the prototype on a printed circuit board (PCB) shown in Fig. 3. The exciting LED (LXZ1-PR01, Lumileds) has a peak wavelength of 450 nm, and the photosensor (SD019-141-411-R, Advanced Photonix) is a silicon PD with an integrated bandpass filter to pass red light with a peak wavelength of 600 nm. To further eliminate the effect of the blue light on the lifetime measurements, we placed a long pass, 550 nm optical filter (Everix, Edmund Optics) on top of the active area of PD. The experimental environment is shown in Fig. 4. We placed the luminescent film inside of an aluminum gas chamber, in which it can interact with the controlled gas mixture. We positioned the prototype above the chamber so that the alignment between the film and both the LED and the PD is proper.

First, we conducted experiments at normal atmospheric conditions near sea level and room temperature to measure the transient response and analyze the effect of LED current and pulse width on the measured lifetime. We varied the LED current and the pulse width from 50 mA to 400 mA in 50 mA steps and from 20 μ s to 200 μ s in 10 μ s steps, respectively. During these experiments, we set the TIA gain to 100 k Ω , and started the sampling 10 μ s before the end of the LED pulse with 2 μ s sampling period, 128 μ s acquisition width (the time frame during which we took samples from the decay curve), and 100 decay curves to be gathered and averaged to reduce the noise in the final data. Also, during the LED current analysis experiment, we measured the dark data without the film at each LED current and stored it to be subtracted from the original data measured with the film for other experiments to eliminate the effect of the blue light further. We ran an exponential regression to calculate τ in MATLAB on the samples collected after 4 μ s at the end of the LED pulse as the blue light effect is still being observed before that.

Then, we conducted a gas experiment with two distinct LED currents and the optimum pulse width determined from previous experiments. We combined the oxygen (OX UHP20, Airgas) and nitrogen (NI UHP80, Airgas) at specific mass flow rates to adjust PO₂ accurately. We adjusted the mass flow

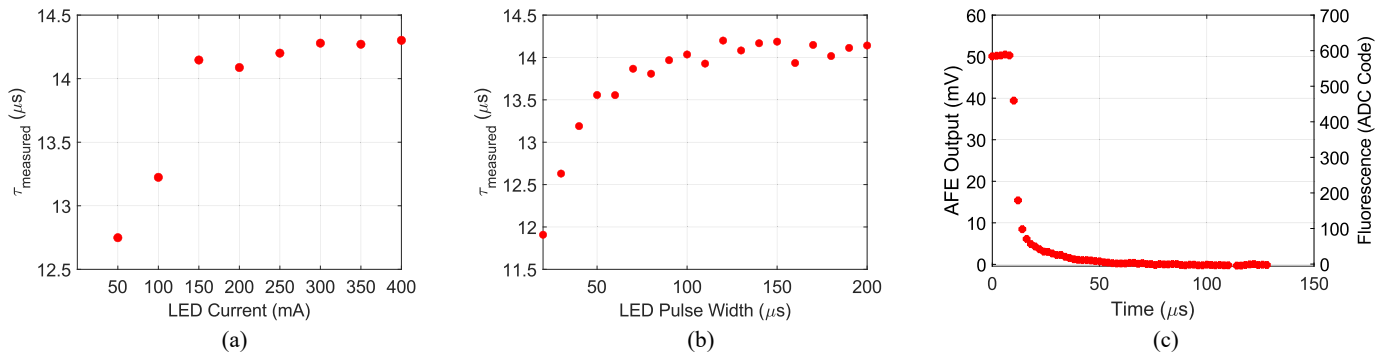


Fig. 5. Effect of a) LED current and b) LED pulse width on lifetime, c) transient response.

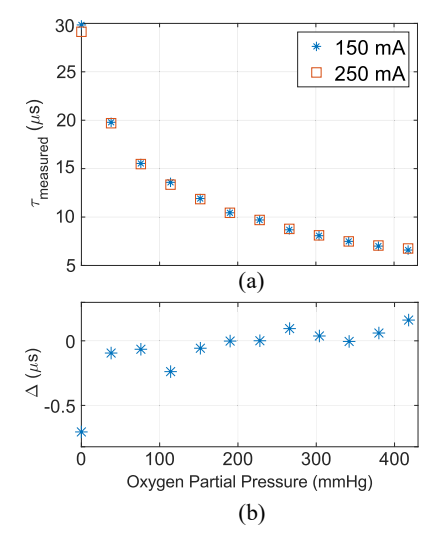


Fig. 6. For 0-418 mmHg range, a) lifetime for two distinct LED currents, b) difference between measured lifetimes.

rates, hence the partial pressure of the test gases, by using two MKS 1179A12CS1BV mass flow controllers (MFCs) and an MKS 247 mass flow control unit. We used the MFC/PC interface to control the whole system via a PC. We changed the PO_2 from 0 to 418 mmHg by varying the oxygen flow rate from 0 to 55 standard cubic centimeters per minute (sccm) while modifying the nitrogen flow rate until the total of the two flow rates equaled 100 sccm at each time.

V. MEASUREMENT RESULTS

We present the results of the LED-current and LED-pulse-width sweep analyses in Fig. 5a and 5b, accordingly. In the LED-current sweep analysis, we observed that τ values reached an asymptote of \sim 14.1 μ s after the 150 mA current point. Moreover, we detected similar behavior in LED pulse width analysis after the 100 μ s point, where τ reached an asymptote. Thus, we can state that 150 mA and 100 μ s are optimal points, matching closely with the results obtained in [30]. The further increase of these parameters beyond these points did not change the τ significantly but increased power consumption. Also, we recorded the transient response with these optimal values, illustrated in Fig. 5c, indicating that the measured response resembles the decay curve of photons.

TABLE I COMPARISON OF PERFORMANCE PARAMETERS

Parameters	[20]	[29]	[21]	This Work
	2021	2022	2021	2022
Supply (V) Max. PD Current (μA)	2.2	1.8 NA	1.2 NA	3 0.4
λ of LED (nm)	453	450	460	450
λ of PD (nm)	600	650	618	600
Power (mW)	9	0.835	0.15	39
Range (mmHg)	0-418	0-228	0-150	0-418

NA: Not Addressed

We performed the gas experiment with 100 μ s LED pulse width for two distinct LED currents, 150 mA and 250 mA. The measured τ ranged from 30 μ s to 6.6 μ s for PO₂ ranging from 0 to 418 mmHg, illustrated in Fig. 6. Based on the literature review, τ does not depend on LED current [20]. Fig. 6b indicates a constant error of less than 0.5 μ s between measured τ of the same PO₂ values. Thus, these results imply that this technique is robust against optical path changes as the LED drive strength does not affect the PO₂ significantly.

We compared the performance parameters of our work to similar works in Table I. [21] consumes the lowest power due to being implemented in a 65 nm technology integrated circuit and fed by a lower supply voltage. Lower power consumption is also reported in [20] since an external function generator is used to drive the LED, and the onboard MCU is not used. The MCU is the most power-hungry component in our prototype due to being ON all the time, which will be reduced by applying an efficient sampling timing scheme and low-power modes in our future work. The presented work sensed a wider PO_2 range compared to [21], [29].

VI. CONCLUSION

We implemented a prototype for continuous noninvasive transcutaneous oxygen monitoring based on the lifetime measurement technique. With the AFE having a 14-bit ADC and the written firmware, we recorded subtle variations in the lifetime, meeting the high-resolution requirement for this technique. To the best of our knowledge, no human subject test using this technique has been presented in the literature. The proposed prototype is a step forward in performing human subject tests with a high-resolution wearable device. Further improvements include developing an algorithm to calculate lifetime onboard and minimizing the power consumption.

REFERENCES

- [1] A. Nag et al., "Wearable flexible sensors: A review," IEEE Sensors Journal, vol. 17, no. 13, pp. 3949-3960, Jul. 2017.
- [2] M. C. Garcia, "Potentially excess deaths from the five leading causes of death in metropolitan and nonmetropolitan counties — United States, 2010-2017," MMWR. Surveillance Summaries, vol. 68, 2019.
- S. Park and S. Jayaraman, "Enhancing the quality of life through wearable technology," IEEE Engineering in Medicine and Biology Magazine, vol. 22, no. 3, pp. 41-48, May 2003.
- "FitBit Fitness Tracker". [Online]. Available: https: //www.fitbit.com/home.
- [5] I. Costanzo et al., "Respiratory monitoring: Current state of the art and future roads," IEEE Reviews in Biomedical Engineering, vol. 15, pp. 103-121, 2022
- [6] SensiumVitals®. [Online]. Available: https://www.sensium.co.uk/.
- [7] Y. A. Bhagat et al., "Like kleenex for wearables: A soft, strong and disposable ECG monitoring system," in 2018 IEEE Biomedical Circuits and Systems Conference (BioCAS), 2018, pp. 1-1.
- [8] I. Tomasic et al., "Continuous remote monitoring of COPD patients-justification and explanation of the requirements and a survey of the available technologies," Medical & Biological Engineering & Computing, vol. 56, no. 4, pp. 547-569, 2018.
- [9] T. Watkins et al., "Nursing assessment of continuous vital sign surveillance to improve patient safety on the medical/surgical unit," J Clin Nurs, vol. 25, no. 1-2, Jan. 2016.
- [10] J.-L. Vincent et al., "Improving detection of patient deterioration in the general hospital ward environment," European Journal of Anaesthesiology, vol. 35, no. 5, pp. 325-333, May 2018.
- [11] U. Guler et al., "Emerging blood gas monitors, how they can help with COVID-19," IEEE Solid-State Circuits Magazine, vol. 12, no. 4, pp. 33-47, 2020.
- [12] P. Grossman, "Respiration, stress, and cardiovascular function," Psychophysiology, vol. 20, no. 3, pp. 284-300, 1983.
- J. E. Hansen, "Arterial blood gases," Clinics in Chest Medicine, vol. 10, no. 2, pp. 227-237, Jun. 1989.
- [14] S. Sharma and M. F. Hashmi, "Partial pressure of oxygen," in *StatPearls*. StatPearls Publishing, Jan. 2022.
- [15] A. K. Verma and P. Roach, "The interpretation of arterial blood gases," Australian Prescriber, vol. 33, no. 4, pp. 124-129, Aug. 2010.
- B. G. Larkin and R. J. Zimmanck, "Interpreting arterial blood gases successfully," AORN Journal, vol. 102, no. 4, pp. 343-357, Oct. 2015.
- [17] A. Umeda et al., "Evaluation of time courses of agreement between minutely obtained transcutaneous blood gas data and the gold standard

- arterial data from spontaneously breathing Asian adults, and various subgroup analyses," BMC Pulmonary Medicine, vol. 20, no. 1, p. 151, May 2020.
- S. Ji et al., "Tuning the luminescence lifetimes of ruthenium(ii) polypyri-[18] dine complexes and its application in luminescent oxygen sensing," Journal of Materials Chemistry, vol. 20, no. 10, pp. 1953-1963, 2010.
- [19] C.-J. Lim et al., "Wearable, luminescent oxygen sensor for transcutaneous oxygen monitoring," ACS Applied Materials & Interfaces, vol. 10, no. 48, pp. 41 026-41 034, Jul. 2018.
- I. Costanzo et al., "A noninvasive miniaturized transcutaneous oxygen monitor," IEEE Transactions on Biomedical Circuits and Systems, vol. 15, no. 3, pp. 474-485, Jun. 2021.
- [21] S. Sonmezoglu et al., "Monitoring deep-tissue oxygenation with a millimeter-scale ultrasonic implant," Nature Biotechnology, vol. 39, no. 7, pp. 855-864, Jul. 2021.
- [22] I. Costanzo et al., "An integrated readout circuit for a transcutaneous oxygen sensing wearable device," in 2020 IEEE Custom Integrated Circuits Conference (CICC), Mar. 2020, pp. 1-4.
- [23] W. van Weteringen et al., "Novel transcutaneous sensor combining optical tcPO2 and electrochemical tcPCO2 monitoring with reflectance pulse oximetry," Med. Biol. Eng. Comput., vol. 58, no. 2, pp. 239-247, Feb 2020.
- [24] J. P. Cascales et al., "Wearable device for remote monitoring of transcutaneous tissue oxygenation," Biomedical Optics Express, vol. 11, no. 12, pp. 6989-7002, Dec. 2020.
- [25] I. Costanzo et al., "Fluorescent intensity and lifetime measurement of platinum-porphyrin film for determining the sensitivity of transcutaneous oxygen sensor," in IEEE International Symposium on Circuits and Systems (ISCAS), Oct. 2020, pp. 1–5. [26] Y.-J. Choi and K. Sawada, "Fluorescence sensors," in Reference Module
- in Biomedical Sciences. Elsevier.
- [27] I. Costanzo et al., "A prototype towards a transcutaneous oxygen sensing wearable," in IEEE Biomedical Circuits and Systems Conference (BioCAS), Oct. 2019, pp. 1-4.
- C. Albrecht, "Principles of fluorescence spectroscopy," Analytical and Bioanalytical Chemistry, vol. 390, no. 5, pp. 1223-1224, Mar. 2008.
- [29] I. Costanzo et al., "A nonuniform sampling lifetime estimation technique for luminescent oxygen measurements," European Solid State Circuits Conference (ESSCIRC), 2022.
- [30] B.Kahraman et al., "Power and accuracy optimization for luminescent transcutaneous oxygen measurements," IEEE International Symposium on Circuits and Systems (ISCAS), pp. 1-4, 2022.
- "ADPD4101 datasheet and product info," [Online]. Available: https:// www.analog.com/en/products/adpd4101.html.